

Review

Explaining Bamboo-Like Carbon Fiber Growth Mechanism: Catalyst Shape Adjustments above Tammann Temperature

Luís Sousa Lobo * and Sónia A.C. Carabineiro 

LAQV-REQUIMTE, Department of Chemistry, NOVA School of Science and Technology, Universidade NOVA de Lisboa, 2829-516 Caparica, Portugal; sonia.carabineiro@fct.unl.pt

* Correspondence: sousalobo266@gmail.com; Tel.: +351-918-266-017

Received: 29 January 2020; Accepted: 23 March 2020; Published: 30 March 2020



Abstract: The mechanism of bamboo-like growth behavior of carbon fibers is discussed. We propose that there is a requirement to have this type of growth: operation above the Tammann temperature of the catalyst (defined as half of the melting point). The metal nanoparticle shape can then change during reaction (sintering-like behavior) facilitating carbon nanotube (CNT) growth, adjusting geometry. Using metal nanoparticles with a diameter below 20 nm, some reduction of the melting point (mp) and Tammann temperature (T_{Ta}) is observed. Fick's laws still apply at nano scale. In that range, distances are short and so bulk diffusion of carbon (C) atoms through metal nanoparticles is quick. Growth occurs under catalytic and hybrid carbon formation routes. Better knowledge of the mechanism is an important basis to optimize growth rates and the shape of bamboo-like C fibers. Bamboo-like growth, occurring under pyrolytic carbon formation, is excluded: the nano-catalyst surface in contact with the gas gets quickly "poisoned", covered by graphene layers. The bamboo-like growth of boron nitride (BN) nanotubes is also briefly discussed.

Keywords: carbon nanotubes; bamboo-like growth; boron nitride nanotubes; kinetics; mechanism

1. Introduction

The mechanism of bamboo-like carbon nanotubes growth requires clarification. A comprehensive review of carbon nanotubes (CNTs) bamboo-like growth has been published recently, covering design, synthesis, and production methods [1]. However, detailed kinetic studies are an efficient key to understand and support a mechanism. This has been demonstrated in catalytic graphene growth [2]. The main scope of the present proposal is to show the need to operate above the Tammann temperature (half of the melting point) to enable bamboo-like growth.

The requirement to have a growth mechanism including carbon (C) atoms bulk diffusion through the metal catalyst nanoparticle excludes bamboo growth from occurring under pyrolytic carbon growth (check Figure 1 and Table 1). The access of C to catalyst bulk operates under catalytic and hybrid carbon formation routes but not in the pyrolytic route, because the whole catalyst surface is covered by graphene layers.

Interstitial bulk diffusion facilitates the catalytic and hybrid C formation mechanisms. An indication of interstitial bulk diffusion being possible is the ratio of the covalent radius of the metal solvent and dissolved atoms (AR_{sol}/AR_{solv}) being less than 0.60. The ratios include C atoms diffusion and N and B atoms diffusion, of interest in boron nitride (BN) nanotubes catalytic growth (point 5, below). Calculation of these ratios is given in Table 2 [3,4]. At higher temperatures, diffusion is much faster. 1st Fick's Law applies: $D = D_0 \exp(-E_d/RT)$; where D the diffusivity, D_0 is maximum diffusion, E_d is the activation energy for diffusion, R is the ideal gas constant and T is temperature. 2nd Fick's law is only of interest initially, until steady-state growth is established [2].

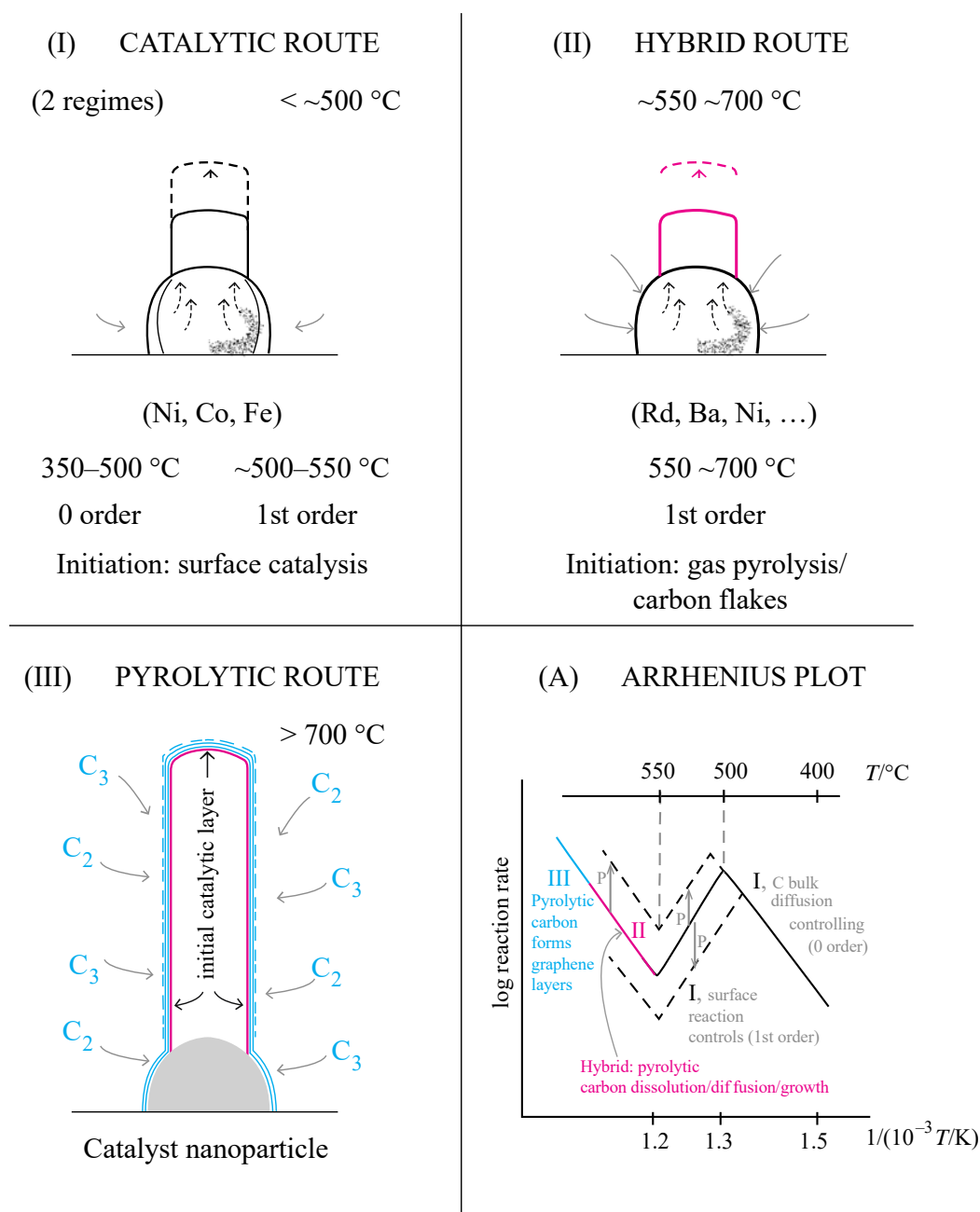


Figure 1. Carbon formation modes: I—Catalytic route; II—Hybrid route; III—Pyrolytic route; A—Evidence of prevailing route from kinetics (Arrhenius plot) observed.

Table 1. Alternative graphene formation routes (see Figure 1, which has the same code of colors).

Kinetic Routes	Temperature Range (°C)	C Growth Type	Active Catalysts
I Catalytic	300–550	Surface catalysis	Fe, Co, Ni
II Hybrid	550–(700)	C black atoms dissolve/grow	Pt, Ru, Mo, Ni, Cu
III Pyrolytic	600–(1200)	C black (C ₂ /C ₃) forms layers	No catalysis, shape adjusts

Table 2. Melting points and Tammann temperatures of 10 metals frequently used in carbon formation and ratios of atomic radius (AR) of solute (C, B, N atoms) and solvent. AR-C = 0.67; AR-N = 0.56; AR-B = 0.87. In most cases $AR_{\text{solute}}/AR_{\text{solvent}} < 0.60$. As a rule, when that ratio is lower than 0.59, interstitial diffusion is easier [3–5].

Metal Solvent	Melting (°C)	T_{Ta} (°C)	AR_{solvent} (pm)	$AR_{\text{solute}}C/AR_{\text{solvent}}$	$AR_{\text{solute}}N/AR_{\text{solvent}}$	$AR_{\text{solute}}B/AR_{\text{solvent}}$
Fe	1538	632	140	0.50	0.36	0.56
Co	1495	611	135	0.52	0.37	0.57
Ni	1455	590	135	0.52	0.38	0.58
Cu	1083	405	135	0.52	0.39	0.60
Ru	2334	1030	130	0.54	0.31	0.49
Rh	1964	845	135	0.52	0.32	0.50
Pd	1555	641	140	0.50	0.33	0.51

The need to enable solid-state shape changes also led to the conclusion that carbon gasification operating above Tammann temperature (T_{Ta}) requires an efficient carbon/catalyst contact and good catalytic activity; effective catalyst nanoparticles show “carbon worm” behavior [6]. Temperatures higher than 550 °C are required and the hybrid route is the usual mechanism operating in bamboo-like carbon growth.

Lee and Park proposed a model assuming base growth [7]. Brown et al. used Pt and microwave plasma operated at 1000 °C, well above T_{Ta} of platinum, obtaining excellent growth of vertically aligned bamboo-like CNTs [8]. Gonzalez et al. studied bamboo-shaped CNTs formation from CH_4 catalyzed by Ni (550–600 °C) and by Cu-Ni (720–830 °C) and discussed the formation mechanism [9,10]. They assumed Ni nanoparticles to be in a *quasi-liquid state*. However, T_{Ta} and surface pressure enable shape modifications in solids. The changes of behavior observed above 640 °C are most probably due to the operations above Tammann temperature of Ni (590 °C) and to the hybrid kinetic regime approaching the pyrolytic carbon formation prevalence.

2. Growth of Carbon Nanotubes above Catalysts Tammann Temperature (T_{Ta})

The different role of the different crystal faces in catalytic carbon growth has been known for decades. Nickel has a face centered structure (fcc) crystal structure. It is known that (111) faces facilitate nucleation and growth. Of the three alternative carbon growth routes (catalytic, hybrid, and pyrolytic—see Table 1) [2], bamboo-like growth is usually a hybrid mechanism, operating above the Tammann temperature of the catalyst particles being used. Values of T_{Ta} for 10 metals are shown in Table 2. Bamboo-like growth is an example of nanoparticle shape changes by solid-solid interaction above T_{Ta} . Crystal shape and crystal orientation of the faces of catalyst nanoparticles is crucial to get a desired shape and a fast rate of growth.

Several authors discussed helical growth of fibers—very frequently observed—based on the catalyst crystal geometry. The dissimilar role of the different crystal faces in carbon growth has been known for decades. A list of publications describing the crystal orientation selectivity for graphene nucleation was included in a previous paper [2]. Shape changes due to contact interaction are facilitated above the Tammann temperature (Figure 2). Bamboo-like growth is a good example of the importance of T_{Ta} in shape adjustment of a nanoparticle by solid-solid interaction.

Zaikovskii et al. claimed that nanoparticle shape changes were due to enhanced fluidity of active metal particles (5–20 nm). This should be understood as a way to refer to the sintering-like behavior [11]. The “fluidity” enabled by T_{Ta} is a superficial phenomenon of the first layer solid-state atoms mobility, under external pressure. Their discussion of the mechanism of CNTs growth observed is clear (Ni/ C_4H_8). However, the suggestion of a cyclic carbide mechanism operating must be ruled out. It is similar to the proposal for solid-state “molecules” operating, used to explain catalytic carbon gasification—which is a misconception [12]. Carbide or any other “external” solid phase may be formed as long as they are in the phase in equilibrium with the gas. Steady-state diffusion is established by adjusting the

thickness of the two phases—an external in equilibrium with the gas and an internal in equilibrium with graphene [1]. As said above, different crystal faces have diverse roles in carbon growth.

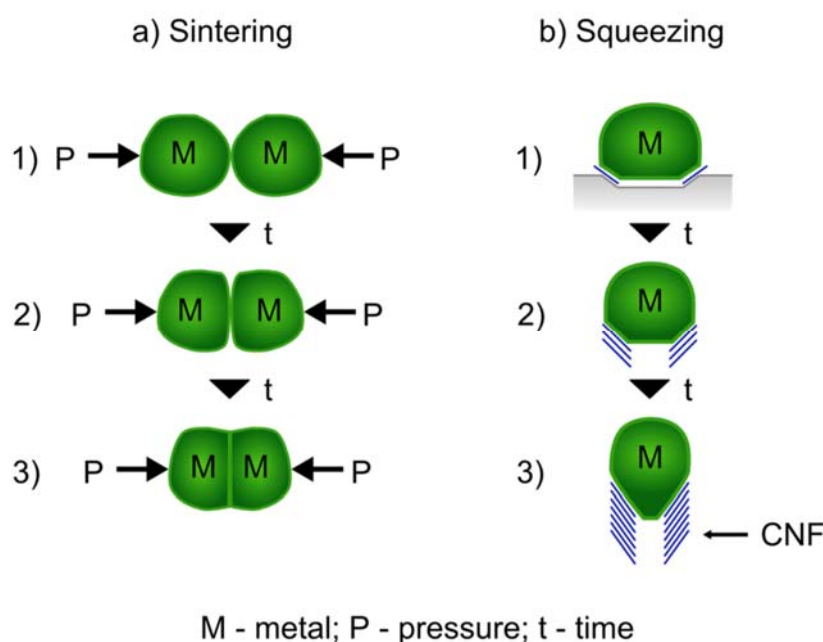


Figure 2. Shape changes of nanoparticles above the Tammann temperature under surface pressure. (a) Sintering under pressure, with time passing (t with arrow) and with the use of pressure (P and arrow signifying where the pressure comes from); (b) Metal nanoparticle changing shape under graphene conical contact pressure, facilitating carbon nanofibers (CNF) growth, with time passing (t with arrow).

Catalyst nanoparticle shape changes have been observed in catalytic carbon growth above the Tammann temperature. Sharma et al. studied the effect of temperature (450–650 °C) and pressure (0.8–20 mTorr) in CNTs formation from C_2H_2 on Ni nanoparticles [13]. Using in situ TEM they observed the change of behavior above ~600 °C. This can be explained by a sintering-like behavior. This has been recently proposed, as remarked above. Sharma et al. found that straight single wall CNTs tend to form at high temperatures and low pressures.

Hofmann et al. studied growth morphologies using very small Ni nanoparticles (2–10 nm) [14]. They observed growth dynamics: elongation and contraction of the catalyst nanoparticle at its tip. The T_{Ta} of very small nanoparticles is lower than for larger nanoparticles/metals. Therefore, the shape dynamics of Ni during graphene growth could be observed below 590 °C with very small Ni particles (T_{Ta} of Ni). Yu et al. gave excellent images and linear kinetics data of CNTs growth using several gases (CO, CO/ H_2 , CH_4 , C_2H_8/H_2) and Fe nanoparticles (5–50 nm) [15]. Liu et al. discussed the change of behavior in view of the lower melting point (and lower T_{Ta}) due to the size of the nanoparticles [16]. The decrease of the melting point occurs below ~20 nm.

We consider that interpreting shape changes of catalyst nanoparticles as due to melting is not correct (as in “Bamboo-like carbon growth due to the effect of melted droplets of metals” [17]). We believe this is not an accurate description of atoms surface mobility, occurring in sintering. Saito et al. used arc discharge in that study. The local conditions of growth (temperature, gas composition, solid phases) are difficult to ascertain.

A quick change of shape of the nanoparticles may occur above the Tammann temperature of the catalyst, facilitating 90° bending. When a new graphene nucleation layer occurs (Figure 3), the required shape change of the catalyst nanoparticle tip takes some time, compared to the CNT growth rate. A 90° bending of the growing graphene layer, bamboo-like growth occurs° as shown in Figure 4. After an initial nucleation, a second nucleation takes time: C concentration on that side of the metal nanoparticle is low.

In Table 3, we list 28 bamboo-like growth studies, including the work of Lee et al. in 2000 (C_2H_2 , Fe, 750–950 °C) [7]. In our view, these authors proposed a correct approach to the mechanism.

Previous studies of Saito (1995) [17] and Li et al. (1999) [18] gave information about growth modes and clues to understand the carbon growth mechanism. Cui et al (2000) discussed bamboo-like growth from methane/ammonia on Fe and its interlayer dependence on reaction temperature (700–950 °C) [19]. A TEM image from their work is shown in Figure 5.

Table 3. A selection of bamboo-like CNTs growth studies. Operating temperatures are always above the Tammann temperature of the metal (see Table 2) facilitating shape adjustment of the particle and 90° turning in graphene growth.

Catalyst	Gas	Temperature (°C)	First Author	Year	Reference
Ni-Cu/Al	CH_4/N_2	500–730	Li YD	1999	[18]
Fe/SiO ₂	C_2H_2	750–950	Lee CJ	2000	[7]
Fe/SiO ₂	CH_4/NH_3	650–950	Cui H	2000	[19]
Ni/Al	CH_4/N_2	500–600	He C	2007	[20]
Ni-Cu/Al ₂ O ₃	CH_4/H_2	720–830	Chen J	2001	[21]
Ni	$C_2H_2/N_2/H_2$	750–950	Jung M	2001	[22]
Ni	Phthalocyanine	600–850	Katayama T	2002	[23]
Fe	Phthalocyanine	1000	Chadderton LT	2002	[24]
Fe,Co,Ni	CH_4/H_2	850–1100	Bartsch K	2005	[25]
Co/Al ₂ O ₃ -Ti	C_2H_2/NH_3	750–950	Jang JY	2006	[26]
Fe	$C_2H_2/NH_3/H_2$	700	Ting JM	2007	[27]
Ni	C_2H_2	650	Lin MT	2007	[28]
Cu	$CH_4/H_2/H_2S$	500–900	Katar SL	2008	[29]
Cu/Al ₂ O ₃	C_2H_5OH	700–850	Xue B	2009	[30]
Ni (AC) ₂	C_4H_4S/H_2-S	Detonation	Wang C	2010	[31]
Ni, Ni-Cu	CH_4/N_2	550–830	Gonzalez I	2011	[9]
Pt/SiO ₂	CH_4/NH_3	1000/Plasma	Brown B	2011	[8]
Cu/Al ₂ O ₃	C_2H_4/He	700–900	Lin JH	2012	[32]
Cu	Ethanol	700–1000	Zhu J	2012	[33]
Fe,Co,Ni,Al ₂ O ₃	C_2H_2	720	Keczenovity E	2013	[34]
Cu/SiO ₂	C_2H_4/He	500–900	Lin YC	2013	[35]
Cu/Al ₂ O ₃	C_2H_2/N_2	550–800	Krishna VM	2014	[36]
La/NiO ₃	Glycerol/Ethanol	700–900	Velasquez M	2014	[37]
Ferrocene/SiO ₂	Dichlorobenzene	800–900	Boi FS	2016	[38]
Ni,Cu,Zn	CH_4	600–800	Saraswat SK	2016	[39]
Fe-Mo/Al ₂ O ₃	$C_3H_4N_2$	800–900	Wang Q	2017	[40]
Fe/Al ₂ O ₃	Polyamide	750	Arnaiz N	2018	[41]
Cobaltocene	Ethanol	500	Tang Y	2018	[42]
Co-Fe/Ru	CO/H_2	750	Kumi DO	2018	[43]

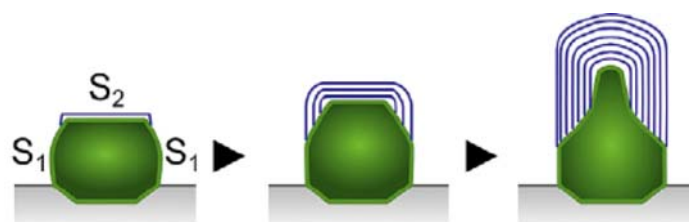


Figure 3. Top growth nucleation with easy sequent C nucleation layers and easy border bending (pentagons). Catalytic C containing gas surface reaction takes place at S1 (lateral “cylindrical” surface). Graphene nucleation occurs at S2 (top flat facet). The graphene layer grows laterally, expanding and bending 90° at the edges of S2 (6 pentagons are required for a perpendicular 90° bending). Sintering-type nanoparticle tip shape adjustments above T_{Ta} enables successive inner nanotubes growth.

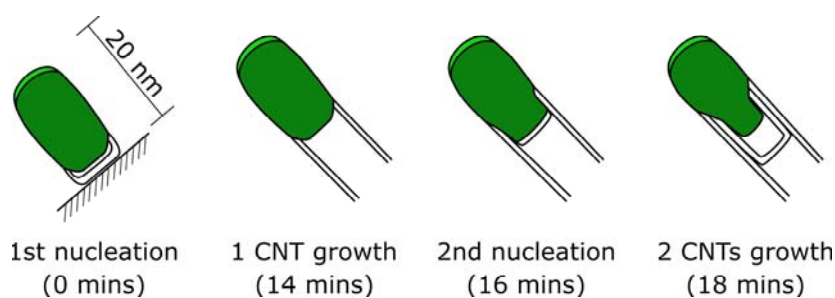


Figure 4. Bamboo-like CNT growth. After a 1st graphene nucleus and 90° bending (6 pentagons) a second nucleation is formed 15 minutes later. This second graphene layer bends after the catalyst nanoparticle readjusts its shape (requirement: $T > T_{Ta}$). The second nucleation takes a few minutes (or seconds, in fast growing systems). Carbon concentration at the narrow end of the nanoparticle is low. A catalytic thin carbide layer active in surface catalysis is not a stable phase at high temperatures.

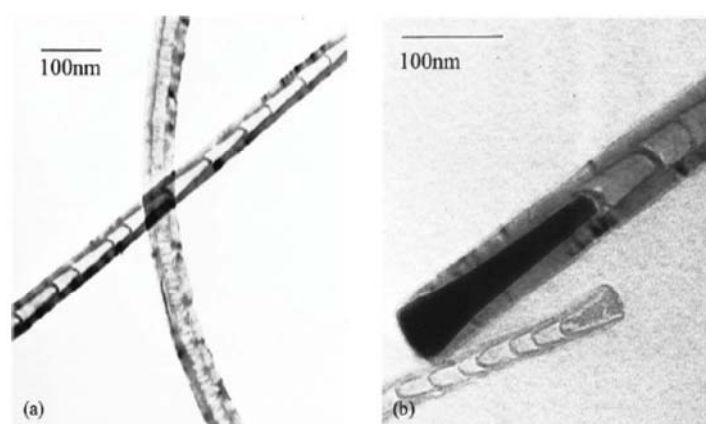


Figure 5. TEM images: (a) Bamboo-like structure; (b) Conical metal particle promoting growth: enabling C nucleation dissolution at the external end and periodic graphene nucleation and growth at the internal end. Reproduced with permission from [19]. Copyright American Institute of Physics, 2000.

3. Alternative Routes and Shapes

Two carbon growth alternatives—octopus carbon (formed at 500 °C) versus bamboo-like (formed at 650 °C)—using the same gas (CH_4/N_2) and the same catalyst (Ni-Cu) demonstrated kinetics and geometry roles. Octopus carbon requires easy and selective carbon nucleation on the eight (111) facets [5]. A scheme of bamboo-like growth initiation is shown in Figure 4

In carbon nanofibers (CNFs) growth, a graphene layer covers the tip and bends in a cylindrical or conical graphene layer, according to catalyst shape. Adjustments in shape of nanocatalysts are possible due to sintering-like reshaping of the metal particle. However, growth of cylindrical CNT structure is not possible when a conical shape prevails. In this case, the structure must include pentagons and heptagons to adjust the growing graphene layer to the conical shape. This shape requires pentagon heptagon pairs or a spiral chirality structure, as discussed by Xu et al. [44]. The crystalline modulus and strength of graphenes versus chirality and shape was discussed. Several properties of conical shaped tubes are very different from those of cylindrical CNTs.

Shape adjustments of the metal nanoparticles require the system to be above the Tammann temperature (T_{Ta}). This can be checked comparing T_{Ta} in Table 1 with the operating temperatures in Table 3. In the case of iron, Fe_3C is usually stable under reaction conditions. The T_{Ta} of iron carbide is lower than the T_{Ta} of iron, which is also listed in Table 1. Table 3 demonstrates that successful experiments to produce bamboo-like nanotubes were run above T_{Ta} . Therefore, catalyst particles can change shape progressively under pressure, as in sintering. At nano scale, the change of shape is much easier. Li et al. used Ni with ~18% Cu [18], which lowers mp and T_{Ta} of Ni-Cu alloy, compared to

pure Ni. Taking a linear adjustment of T_{Ta} of each metal to alloy proportions, one obtains ~ 560 °C for T_{Ta} of that particular Ni-Cu alloy composition.

In fact, lower melting points of alloys can be used to facilitate bamboo-like growth. There are two alternatives for the mp of the alloy: either between the mp of the two metals, varying linearly with composition (e.g., Cu-Ni), or lower than both metals, when an eutectic phase diagram applies (e.g., Cu-Ag). This leads to a lower mp in both cases and so a lower T_{Ta} as well ($\Delta T_{Ta} = \frac{1}{2} \Delta mp$).

Detailed studies by Merkulov et al. covered bamboo-like growth [45–48]. Their search for a mechanism was usually based on physics (e.g., balance of forces). Becker et al. studied CNTs growth with Co-Mn alloys using C_2H_2/H_2 [49]. The T_{Ta} of Mn is 486 °C. For the 50% Co-Mn alloy, T_{Ta} can be estimated as 0.50 of the alloy mp in the phase diagram. That mp is ~ 1200 °C and so T_{Ta} should be 463 °C. Bamboo-like behavior observed at 550 °C is thus explained. Using a glow discharge method, Merkulov et al. obtained thin conical structures (CNCs) with C_2H_2 and NH_3 on Ni, at an estimated temperature of 750 °C [45–48]. This growth could be a variant of a pyrolytic route, based on the addition of C atoms (C_2 - C_3).

The sintering-like behavior required for metallic catalyst nanoparticle shape adjustments, to allow graphene 90° bending and further growth, is understood. The progressive narrower diameter of inner cylindrical core and the attrition between the cylindrical metal nanoparticle extension and the multiwall CNT sliding during growth explains cylindrical metal pieces observed inside long CNTs.

Cui et al. discussed the growth mechanism: time lag between re-nucleation, geometry details of growth—individual bamboo sections terminating inside or outside the larger multiwall structural series of stacked cones [19]. They proposed that “the re-nucleated tip sections are continuous to the point where they terminate on the outer walls of the tube, forming a series of stacked cones”.

In a recent article, Maurice et al. discuss the growth mode operating in bamboo-like growth. They studied growth of graphene layers at the surface of Fe_3C nanoparticles by in situ TEM, using plasma enhanced chemical vapor deposition [50]. T_{Ta} of cementite is 475 °C, somewhat lower than Fe (check Table 1). This facilitates the sintering-like shape changes. Formation of new graphene layers was observed “below” the previous one. Facets on the catalyst nanoparticle were developed, as well as elongation and retraction of the shape of the nanoparticle due to lateral pressure, very similar to the case of bamboo-like growth. They distinguished a “collective” type of CNT growth and “onion” type carbon nano-fiber growth. This layering is similar to the case shown in Figure 6, taken from the work of He et al. [20]. This study helps to understand the sintering-like changes at the surface of solid particles, facilitated at nano scale. The C deposition mechanism operating should be seen as a hybrid route type [2]. This behavior should not be described as melting of the catalyst. Tammann temperature is half of the melting point (in K), as said above, and offers a good basis to understand bamboo-like graphene growth. Bamboo-like CNTs are now being produced for use in important applications [1].

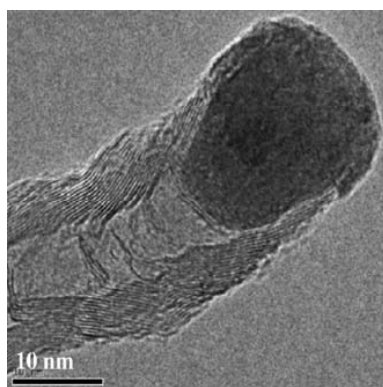


Figure 6. Bamboo-like growth: details of the graphene layers successively nucleating at the flat top of the catalyst particle and growing along the conical lateral surface below the precedent graphene layer. Reprinted from [20], Copyright (2007), with permission from Elsevier.

Jung et al. [22] studied CNTs including bamboo-like growth using Ni as catalyst with $C_2H_2/N_2/H_2$ gas mixtures at 850 °C. They observed: “Lower decomposition rate of C_2H_2 seems to prevent the passivation of the catalyst of the catalyst surface caused by excessive carbon deposition, which in turn enhances the growth of CNT”. We may conclude that the rate-determining step must be the (slower) surface C deposition. Otherwise the catalyst surface will be fully covered with carbon layers and “hybrid” catalytic carbon growth is no longer possible.

Kovalevsky et al. [51] studied C formation and growth behavior from C_2H_2 , C_6H_6 (benzene) and C_2H_4 on Fe, Co, and Ni at high temperatures. Their study included the growth of carbon layers into a cavity, hollow carbons on melted and evaporated catalyst particles, bursting of shells, bamboo-like fibers, and CNTs growth. Xue et al. studied bamboo-like growth, using Cu/Al_2O_3 and methanol in the 700–850 °C temperature range [30]. Bartsch et al. studied CNTs and bamboo-like growth in the range 900–1100 °C using CH_4 . They assumed liquid particle growth during tubular multi-walled carbon nanotubes (MWCNTs) tip growth, as well as molten surface layer during bamboo-like growth at 900 °C [25,52]. These melting assumptions are misleading.

Shape changes under contact pressure above T_{Ta} are well known. The mechanism prevailing must be pyrolytic. This is still possible above 1000 °C when the CH_4 partial pressure is low (0.3 to 1.6 % in this case), so that carbon atoms bulk diffusion is still the faster kinetic step. They observed that growth stops earlier at higher CH_4 partial pressures, as expected, considering pyrolytic carbon impingement to cover the nano-catalyst external surface. In this case, C bulk diffusion cannot be the “rate-controlling step”: the surface is rapidly covered with carbon, blocking C atoms access to bulk diffusion. A study of CNTs was based on schematic geometry alternatives, including bamboo-like growth [53]. However, solid-state chemistry and detailed kinetic studies are the keys to discover prevailing mechanisms in given conditions.

Harris summarized earlier proposals of VLS (vapor–liquid–solid) mechanisms [54]. Liquefying effects are sometimes mentioned. More proposals in that perspective have been published recently. We think those approaches are misleading. It is well known that shape changes occur under contact pressure in solids above T_{Ta} . The facilitating effect of sulfur has been known for some time and studied in more detail recently by Wang et al. [31]. A 1998 study from Wu and Sahajwalla, using Fe and dealing with this effect was mentioned, but it was performed at 1600 °C (above the melting point of Fe) [55]. Several groups have developed methods to grow CNTs, including bamboo-like ones, based on detonation-assisted processes [56,57]. Shaikjee and Coville discussed in detail the role of the carbon source on the types of growth of carbon materials [58].

4. Opening and Filling Observed in MWCNTs

An introduction to filling carbon nanotubes studies can also be found in Harris textbook [54]. In a 2006 study by Sun et al., carbon nanotube formation from ethanol or toluene in the range of temperatures 600–850 °C using electron irradiation experiments was followed using in situ TEM observations [59]. The authors described the changes as shrinkage or thinning of the inner core (nano-catalyst metal particle), and the high strength of the carbon nanotubes against internal pressure—“operating” as high-pressure cylinders and nanoextruders of nano-catalyst particles of Fe, Fe_3C , and Co. However, a sintering-like shape changing mechanism explains well the observed behavior, involving metal atoms surface and sub-surface self-diffusion. Changes in shape were similar to the observed for bamboo-like growth catalyst. In a previous similar 1994 study, Amelinckx et al. used acetylene or benzene and Co, Fe or Ni nanoparticles (~5 nm diameter) on SiO_2 at 600–700 °C. The observed growth behavior was explained using the concept of a spatial-velocity holograph [60]. “Extrusion” is not a correct description of hybrid CNT formation (route II) prevailing in the temperature range used (600–700 °C) [59]. This concept avoids kinetics, which is the main key to discover which mechanism is operating. We believe that sintering-like behavior above the Tammann temperature is the more plausible explanation for the observed behavior (check Table 2, Fe: T_{Ta} = 632 °C; below 20 nm diameter mp/T_{Ta} are lower). Shape changes are due to atom adjustments at the surface or

just below the surface of the catalyst nanoparticle. This sintering-like behavior is certainly easier and faster at nano scale. The shape elongation of the cylindrical part of the catalyst is due to the successive thinner CNTs growing. The separation of cylindrical metal tips is a consequence of the interface attrition between metal and internal graphene nanotube layer growing. In a sintering-like mechanism, shape changes of catalyst nanoparticles are facilitated by surface and sub-surface diffusion of metal atoms. Velasquez et al. [40] studied carbon formation from a methanol/glycerol mixture using LaNiO_3 as a catalyst in the 700–900 °C range. At 800–900 °C, bamboo-like growth was observed. Metal particles were observed inside the CNTs. Usman et al. studied the formation of N-doped MWCNTs. A bamboo-like structure and cylindrical Fe nanoparticles embedded inside were also observed by Coville and co-workers [61] and included in a comprehensive review of carbon growth alternatives [62].

5. Bamboo-Like Hexagonal Boron Nitride (h-BN) Nanotubes and Thin Films

Boron nitride nanotubes have been grown successfully in recent years [63–66]. The structure of h-BN is formed by a hexagonal atom structure in layers similar to graphite but with $3 \times \text{N} + 3 \times \text{B}$ atoms (alternating) in each hexagon, instead of six carbon atoms. The growth mode and bamboo-like growth mechanisms should be similar to CNTs growth. The easy diffusion of carbon through the catalyst nanoparticle must be interstitial due to the ratio of the covalent radius of solvent (Fe) and solutes (N, B), as demonstrated by Barrer [4] (check Table 2). C, N or B atoms bulk diffusion through the catalyst nanoparticles is the key to supply atoms to get nucleation and grow well-ordered nanotubes. The formation of six pentagons in a new growing layer to change to a perpendicular growth with CNTs must have a similar solution in BN tubes growth.

Zhang et al. [65] observed bamboo-like growth by electron microscopy, as seen in Figure 7.

A survey of the growth types observed is available (Wang, et al. [66]). The geometry of active particles demonstrates the nucleation and growth mechanism. The operating shape of active catalyst nanoparticles is a key factor in the growth process and in BN geometry, structure, and physical properties.

Recently, carbon CB and CN thin films have been produced exhibiting interesting properties [67,68]. The atomic structure of CN, CN and BN films is shown in Figure 8 [64]. Carbon oxide films have also been prepared and show very useful properties [69–71], but in this case the 2D layers are not just hexagonal graphene-like structures. Oxide semiconductor thin-film transistors (TFT) is a very active area presently, with great progress in electronic devices production [69–71]. Carbon spheres (CSs) have been produced and tested as super capacitors, as an alternative to other structures (vg. carbon thin films) [72–75].

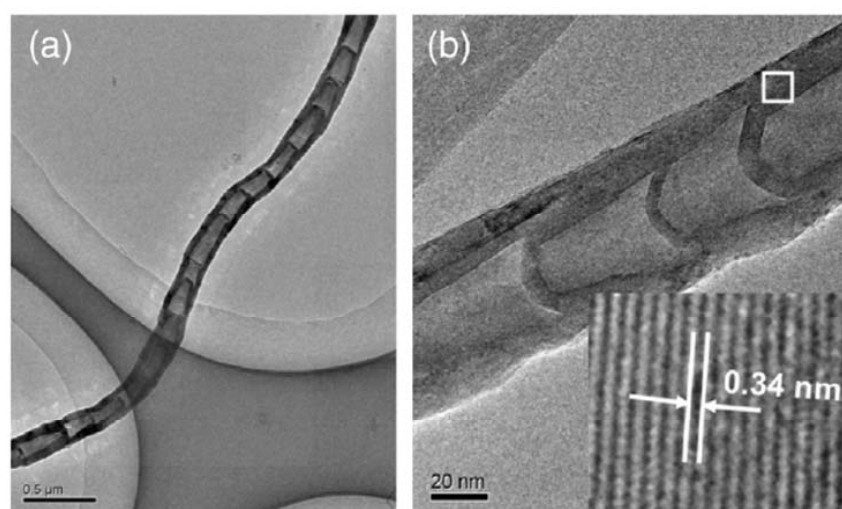


Figure 7. TEM images: BN (boron nitrite) nanotubes showing bamboo-like growth. Reprinted from [65], Copyright (2012), with permission from Elsevier.

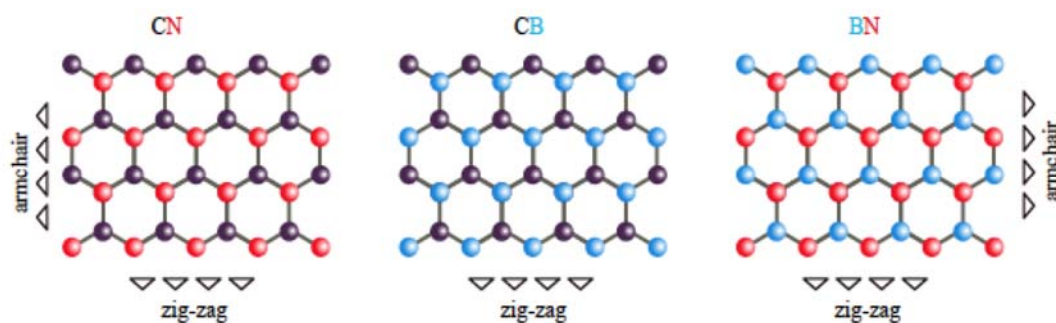


Figure 8. Structure of CN, CB, and BN thin films

6. Conclusions

1. Bamboo-like growth behavior of carbon fibers occurs most likely by a sintering-like shape change of the catalyst particles, enabling a new graphene layer to bend and grow further (inside the growing structure). This is possible above the Tamman temperature of the metal particle under catalytic (I) or hybrid (II) carbon growth routes, but not under pyrolytic (III) growth. Shape changes are not due to liquefaction but to movements of the metal atoms of the external layer of the catalyst nanoparticle—under surface contact pressure.

2. This sintering-like behavior should not be described as melting or liquid-like. Catalysis by solids is based on a surface structure: liquids do not have a stable surface structure.

3. Kinetics is an important key to understand the behavior observed, particularly the concept of rate-determining step. Isothermal kinetic studies are required. Scanning temperature studies give useful initial information. However, reaction orders and activation energy evaluation in new systems require isothermal experiments. “Optimizing industrial production of carbon nanotubes is an important objective nowadays. Knowing the mechanisms operating helps to control properties, optimize production and reduce costs more easily” [76].

4. The use of alloy nano-catalyst may lower the melting point and T_{Ta} . There are two alternative alloy phase diagrams concerning the alloy melting point (mp): a) Exhibiting linear variation of mp with composition; b) Exhibiting an eutectic dependence and thus showing a clear decrease of mp with the right alloy composition.

5. Catalytic Growth of CNTs and also BN, CB, or CN nanotubes is possible because of the easy bulk diffusion of these atoms (C, B, N) through the solid-state structure of quite a few transition metals, which is facilitated by interstitial diffusion (Table 2).

Author Contributions: L.S.L. performed the literature search and wrote the paper. S.A.C.C. revised and edited the manuscript. All authors have read and agreed to the published version of the manuscript.

Funding: This work was supported by the Associate Laboratory for Green Chemistry—LAQV which is financed by national funds from FCT/MCTES (UIDB/50006/2020).

Acknowledgments: The authors thank Victor Teodoro for the help with the drawings.

Conflicts of Interest: The authors declare no conflict of interest.

References

1. Jia, Z.; Kou, K.; Qin, M.; Wu, H.; Puleo, F.; Liotta, F. Controllable and large-scale synthesis of carbon Nanostructures: A Review of Bamboo-Like Nanotubes. *Catalysts* **2017**, *7*, 256. [CrossRef]
2. Lobo, L.S. Catalytic carbon formation: Clarifying the alternative kinetic routes and defining a kinetic linearity for sustained growth concept. *React. Kinet. Mech. Cat.* **2016**, *118*, 393–414. [CrossRef]
3. Barrer, R.M. Aspects of gas-metal equilibrium, interstitial solution and diffusion. *Discuss. Faraday Soc.* **1948**, *4*, 68–81. [CrossRef]
4. Barrer, R.M. *Diffusion in and through Solids*; The University Press, MacMillan: Cambridge, UK, 1941.

5. Cordero, B.; Gomez, V.; Platero-Prats, A.E.; Revés, M.; Echeverria, J.; Cremades, E.; Barragán, F.; Alvarez, S. Covalent radii revisited. *Dalton Trans.* **2008**, 2832–2838. [[CrossRef](#)] [[PubMed](#)]
6. Lobo, L.S.; Carabineiro, S.A.C. Kinetics and mechanism of catalytic carbon gasification. *Fuel* **2016**, *183*, 457–469. [[CrossRef](#)]
7. Lee, C.J.; Park, J. Growth model of bamboo-shaped carbon nanotubes by thermal chemical vapor deposition. *Appl. Phys. Lett.* **2000**, *77*, 3397–3399. [[CrossRef](#)]
8. Brown, B.; Parker, C.B.; Stoner, B.R.; Glass, J.T. Growth of vertically aligned bamboo-like carbon nanotubes from ammonia/methane precursors using a platinum catalyst. *Carbon* **2011**, *49*, 266–274. [[CrossRef](#)]
9. Gonzalez, I.; de Jesus, J.C.; Canizales, E. Bamboo-shaped CNTs generated by methane thermal decomposition using Ni nanoparticles synthesized in water-oil emulsions. *Micron* **2011**, *42*, 819–825. [[CrossRef](#)]
10. De Jesus, J.C.; Gonzalez, I.; Garcia, M.; Urbina, C. Preparation of nickel nanoparticles and their catalytic activity in the cracking of methane. *J. Vac. Sci. Technol. A* **2008**, *26*, 913–918. [[CrossRef](#)]
11. Zaikovski, V.I.; Chesnokov, V.V.; Buyanov, R.A. The Relationship between the State of Active Species in a Ni/Al₂O₃ Catalyst and the Mechanism of Growth of Filamentous Carbon. *Kinet. Catal.* **2001**, *42*, 890–931. [[CrossRef](#)]
12. McKee, D.W. Metal oxides as catalysts for oxidation of graphite. *Carbon* **1970**, *8*, 623–626. [[CrossRef](#)]
13. Sharma, R.; Rez, P.; Brown, M.; Du, G.; Treacy, M.M.J. Dynamic observations of the effect of pressure and temperature conditions on the selective synthesis of carbon nanotubes. *Nanotechnology* **2007**, *18*, 125602–125609. [[CrossRef](#)]
14. Hofmann, S.; Sharma, R.; Ducati, C.; Du, G.; Mattevi, C.; Cepek, C.; Cantoro, M.; Pisana, S.; Parvez, A.; Cervantes-Sodi, F.; et al. In situ observations of Catalyst Dynamics during Surface-Bound Carbon Nanotube Nucleation. *Nano Lett.* **2007**, *7*, 603–608. [[CrossRef](#)] [[PubMed](#)]
15. Yu, Z.; Chen, D.; Totdal, B.; Holmen, A.H. Effect of support and Reactant on the Yield and Structure of Carbon Growth by Chemical vapor deposition. *J. Phys. Chem. B* **2005**, *109*, 6096–6102. [[CrossRef](#)] [[PubMed](#)]
16. Liu, H.B.; Ascensio, J.A.; Perez-Alvarez, M.; Yacaman, M.J. Melting behavior of nanometer sized gold isomers. *Surf. Sci.* **2001**, *491*, 88–98. [[CrossRef](#)]
17. Saito, Y. Nanoparticles and filled nanocapsules. *Carbon* **1995**, *33*, 979–988. [[CrossRef](#)]
18. Li, Y.D.; Chen, J.; Ma, Y.; Zhao, J.; Qin, Y.; Chang, L. Formation of bamboo-like nanocarbon and evidence for the quasi-liquid state of nanosized metal particles at moderate temperatures. *Chem. Comm.* **1999**, 1141–1142. [[CrossRef](#)]
19. Cui, H.; Zhou, O.; Stoner, B.R. Deposition of aligned bamboo-like carbon nanotubes via microwave plasma enhanced chemical vapor deposition. *J. Appl. Phys.* **2000**, *88*, 6072–6074. [[CrossRef](#)]
20. He, C.; Zhao, N.; Shi, C.; Du, X.; Li, J. TEM studies of the initial stage growth and morphologies of bamboo-shaped carbon nanotubes synthesized by CVD. *J. Alloys Comp.* **2007**, *433*, 79–83. [[CrossRef](#)]
21. Chen, J.; Li, Y.; Ma, Y.; Qin, Y.; Chang, L. Formation of bamboo-shaped carbon filaments and dependence of their morphology on catalyst composition and reaction conditions. *Carbon* **2001**, *39*, 1467–1475. [[CrossRef](#)]
22. Jung, M.; Eun, K.Y.; Lee, J.-K.; Baik, Y.-J.; Lee, K.-R.; Park, J.W. Growth of CNTs by CVD. *Diamond Rel. Mater.* **2001**, *10*, 1235–1240. [[CrossRef](#)]
23. Katayama, T.; Araki, H.; Yoshino, K. Multiwalled nanotubes with bamboo-like structure and effects of heat treatment. *J. Appl. Phys.* **2002**, *91*, 6675–6678. [[CrossRef](#)]
24. Chadderton, L.T.; Chen, Y. A model for the growth of bamboo and skeletal nanotubes: Catalytic capillarity. *J. Crystal Growth* **2002**, *240*, 164–169. [[CrossRef](#)]
25. Bartsch, K.; Biedermann, J.; Gemming, T.; Leonhardt, A. On the diffusion-controlled growth of multi-walled CNTs. *J. Appl. Phys.* **2005**, *97*, 114301. [[CrossRef](#)]
26. Jang, Y.; Lee, C.E.; Lee, T.J.; Lyu, S.C.; Lee, C.J. Lateral force microscopy of bamboo-shaped multiwalled CNTs. *Curr. Appl. Phys.* **2006**, *6*, 141–144. [[CrossRef](#)]
27. Ting, J.-M.; Lin, S.-H. Growth and characteristics of CNTs obtained under different C₂H₂/H₂/NH₃ concentrations. *Carbon* **2007**, *45*, 1934–1940. [[CrossRef](#)]
28. Lin, M.T.; Tan, J.P.I.; Boothroyd, C.; Loh, K.P.; Tok, E.S.; Foo, Y.-L. Dynamical Observation of Bamboo-like Carbon Nanotube Growth. *Nano Lett.* **2007**, *7*, 2234–2238. [[CrossRef](#)]
29. Katar, S.L.; Gonzalez-Berrios, A.; de Jesus, J.; Weiner, B.; Morell, G. Direct deposition of Bamboo-Like Carbon Nanotubes on Copper Substrates by Sulfur-Assisted HFCVD. *J. Nanomat.* **2008**. article 515890 (7 pages). [[CrossRef](#)]

30. Xue, B.; Liu, R.; Huang, W.-Z.; Zheng, Y.-F.; Xu, Z.-D. Growth and characterization of bamboo-like multiwalled carbon nanotubes over Cu/Al₂O₃ catalyst. *J. Mater. Sci.* **2009**, *44*, 4040–4046. [[CrossRef](#)]
31. Wang, C.; Zhan, L.; Wang, Y.-L.; Qiau, W.-M.; Liang, X.; Ling, L.-C. Effect of Sulfur on the growth of carbon nanotubes by detonation-assisted CVD. *Appl. Surf. Sci.* **2010**, *257*, 932–936. [[CrossRef](#)]
32. Lin, J.-H.; Chen, C.-S.; Zheng, Z.-Y.; Chang, C.-W.; Chen, H.-W. Sulphate-activated growth of bamboo-like carbon nanotubes over copper catalysts. *Nanoscale* **2012**, *4*, 4757–4764. [[CrossRef](#)] [[PubMed](#)]
33. Zhu, J.; Jia, J.; Kwong, F.; Ng, D.H.L. Synthesis of bamboo-like CNTs on a Cu foil by catalytic CVD from ethanol. *Carbon* **2012**, *50*, 2504–2512. [[CrossRef](#)]
34. Keczenovity, E.; Fejes, D.; Reti, B.; Hernadi, K. Growth and characterization of bamboo-like carbon nanotubes synthesized on Fe–Co–Cu catalysts prepared by high-energy ball milling. *Phys. Status Solidi B* **2013**, *250*, 2544–2548. [[CrossRef](#)]
35. Lin, Y.C.; Lin, J.H. Purity-controllable growth of bamboo-like multi-walled CNTs over copper-based catalysts. *Catal. Commun.* **2013**, *34*, 41–44. [[CrossRef](#)]
36. Krishna, V.M.; Abilarassu, A.; Somanathan, T.; Gokulakrishnan, N. Effective synthesis of well graphitized high yield bamboo-like MWCNTs on copper loaded α -alumina nanoparticles. *Diamond Rel. Mater.* **2014**, *50*, 20–25. [[CrossRef](#)]
37. Velasquez, M.; Batiot-Dupeyrat, C.; Gallego, J.; Santamaria, A. Chemical and morphological characterization of MWCNTs synthesized by C deposition from ethanol-glycerol blend. *Diamond Rel. Mater.* **2014**, *50*, 30–48. [[CrossRef](#)]
38. Boi, F.S.; Wang, S.; He, Y. Mapping the transition from catalyst-pool to bamboo-like growth-mechanism in VA free-standing films of CNTs filled with Fe₃C: The key role of water. *AIP Adv.* **2016**, *6*, 0851012016. [[CrossRef](#)]
39. Sarawast, S.K.; Sinha, B.; Pant, K.K.; Gupta, R.B. Kinetic Study and Modeling of Homogeneous Thermocatalytic Decomposition of Methane over a Ni-Cu-Zn/Al₂O₃ Catalyst for the Production of Hydrogen and Bamboo-Shaped CNTs. *Ind. Eng. Chem. Res.* **2016**, *55*, 11672–11680. [[CrossRef](#)]
40. Wang, Y.; McIntyre, P.C.; Cai, W. Phase Field Model for Morphological Transition in Nanowire Vapor-Liquid-Solid Growth. *Crystal Growth Des.* **2017**, *17*, 2211–2227. [[CrossRef](#)]
41. Arnaiz, N.; Martin-Gullon, I.; Font, R.; Gomez-Rico, M.F. Production of bamboo-type carbon nanotubes doped with nitrogen from polyamide pyrolysis gas. *J. Anal. Appl. Pyrol.* **2018**, *130*, 52–61. [[CrossRef](#)]
42. Tang, Y.; Luo, W. Synthesis and Characterization of Bamboo-like MWCNTs By Alcohothermal Process. *IOP Conf. Ser. Earth Environ. Sci.* **2018**, *186*, 012058. [[CrossRef](#)]
43. Kumi, D.O.; Phaahlamohlaka, T.N.; Dlamini, M.W.; Mangezvo, I.T.; Mhlanga, S.D.; Scurrrell, M.S.; Coville, N.J. Effect of titania covering on CNTs as support for the Ru catalyzed selective Co metanation. *Appl. Cat. B Environ.* **2018**, *232*, 492–500. [[CrossRef](#)]
44. Xu, F.-F.; Bando, Y. Structures of a hollow filamentary conical helix. *Acta Cryst. A* **2003**, *59*, 168–171. [[CrossRef](#)] [[PubMed](#)]
45. Merkulov, V.I.; Guillom, M.A.; Lowndes, D.H.; Simpson, M.L.; Voelkl, E. Shaping carbon nanostructures by controlling the synthesis process. *Appl. Phys. Lett.* **2001**, *79*, 1178–1180. [[CrossRef](#)]
46. Merkulov, V.I.; Hensley, D.K.; Melechko, A.V.; Guillorn, M.A.; Lowndes, D.H.; Simpson, M.L. Control Mechanisms for the Growth of Isolated Vertically Aligned Carbon Nanofibers. *J. Phys. Chem. B* **2002**, *106*, 10570–10577. [[CrossRef](#)]
47. Melechko, A.V. Vertically aligned CNF and related structures: Controlled synthesis and directed assembly. *J. Appl. Phys.* **2005**, *97*, 041301. [[CrossRef](#)]
48. Merkulov, I.A.; Yoon, M.; Geoghegan, D.B. How the shape of catalyst nanoparticles determines their crystallographic orientation during carbon nanofiber growth. *Carbon* **2013**, *60*, 41–45. [[CrossRef](#)]
49. Becker, M.J.; Xia, W.; Tessonier, J.-P.; Blume, R.; Yao, L.; Schlögl, R.; Muhler, M. Optimizing the synthesis of cobalt-based catalysts for the selective growth of multiwalled CNTs under industrially relevant conditions. *Carbon* **2011**, *49*, 5253–5264. [[CrossRef](#)]
50. Maurice, J.-L.; Pribat, D.; He, Z.; Patriarche, G.; Cojocaru, C.S. Catalyst faceting during graphene layer crystallization in the course of carbon nanofiber growth. *Carbon* **2014**, *79*, 93–102. [[CrossRef](#)]
51. Kovalevski, V.V.; Safronov, A.N. Pyrolysis of Hollow Carbons Melted Catalyst. *Carbon* **1998**, *36*, 963–968. [[CrossRef](#)]
52. Bartsch, K.; Leonhardt, A. An approach to the structural diversity of aligned grown multi-walled CNTs on catalyst layers. *Carbon* **2004**, *42*, 1731–1736. [[CrossRef](#)]

53. Mohammad, S.N. Systematic investigation of the growth mechanism for conventional, doped and bamboo-shaped nanotubes. *Carbon* **2014**, *75*, 133–148. [[CrossRef](#)]
54. Harris, P.J.F. *Carbon Nanotube Science: Synthesis, Properties and Applications*; Cambridge University Press: Cambridge, UK; New York, NY, USA, 2011.
55. Wu, C.; Sahajwalla, V. Influence of Melt Carbon and Sulfur on the Wetting of Solid Graphite by Fe-C-S Melts. *Metallurg. Mater. Trans. B* **1998**, *29*, 471–477. [[CrossRef](#)]
56. Luo, N.; Jiu, H. Gaseous detonation fabrication of CNTs and CNTs doping with Fe based composites. *Fuller. Nanotub. Carb. Nanostruct.* **2016**, *24*, 494–499. [[CrossRef](#)]
57. Lu, Y.; Zhu, Z.; Wu, W.; Liu, Z. Detonation chemistry of a CHNO explosive: Catalytic assembly of carbon nanotubes at low pressure and temperature state. *Chem. Commun.* **2002**, 2740–2741. [[CrossRef](#)]
58. Shaikjee, A.; Coville, N.J. The role of the hydrocarbon source on the growth of carbon materials. *Carbon* **2012**, *50*, 33376–33398. [[CrossRef](#)]
59. Sun, L.; Banhart, F.; Krashennnikov, A.V.; Rodrigues-Manzo, J.A.; Terrones, H.; Ajyan, P.M. Carbon nanotubes as high-pressure cylinders and nanoextruders. *Science* **2006**, *312*, 1199–1202. [[CrossRef](#)]
60. Amelinckx, S.; Zhang, X.B.; Bernaerts, D.; Zhang, X.F.; Ivanov, V.; Nagy, B.A. Formation Mechanism for Catalytically Grown Helix-Shaped Graphite Nanotubes. *Science* **1994**, *265*, 635–639. [[CrossRef](#)]
61. Usman, I.B.; Matsoso, M.; Ranganathan, K.; Naidoo, D.; Coville, N.J.; Wamwangi, D. Magnetic properties of iron containing N-doped MWCNTs. *Mater. Chem. Phys.* **2018**, *209*, 280–290. [[CrossRef](#)]
62. Coville, N.J.; Mhlanga, S.D.; Nxumalo, E.N.; Saikjee, A. A review of shaped carbon nanomaterials. *S. Afr. J. Sci.* **2011**, *107*, 1–15. [[CrossRef](#)]
63. Han, W.; Bando, Y.; Kurashima, K.; Sato, T. Synthesis of boron nitride nanotubes from carbon nanotubes by a substitution reaction. *Appl. Phys. Lett.* **1998**, *73*, 3085–3087. [[CrossRef](#)]
64. Ma, Y.; Bando, Y.; Sato, T. Controlled Synthesis of BN Nanotubes, Nanobamboos and Nanocables. *Adv. Mater.* **2002**, *14*, 366–368. [[CrossRef](#)]
65. Zhang, L.; Wang, J.; Gu, Y.; Zhao, G.; Qian, Q.; Li, J.; Pan, X.; Zhang, Z. Catalytic growth of bamboo-like boron nitride nanotubes using self-propagation HT synthesized porous precursor. *Mater. Lett.* **2012**, *67*, 17–20. [[CrossRef](#)]
66. Wang, J.; Zhang, L.; Zhao, G.; Gu, Y.; Zhang, Z. Selective synthesis of boron nitride nanotubes by self-propagation high temperature synthesis and annealing process. *J. Solid State Chem.* **2011**, *184*, 2478–2484. [[CrossRef](#)]
67. Sharma, B.B.; Parashar, A. A review on thermo-mechanical properties of bi-crystalline and polycrystalline 2D nanomaterials. *Crit. Rev. Solid State Mater. Sci.* **2019**, *45*, 134–170. [[CrossRef](#)]
68. Yu, B.-S.; Ha, T.-J. High-performance Solution-Processed IGZO Thin-Film Transistors with Al₂O₃/BN Composite dielectrics Fabricated at Low Temperature. *Phys. Status Solidi A* **2018**, *215*, 1700802. [[CrossRef](#)]
69. Zhu, Y.; Murali, S.; Cai, W.; Li, X.; Suk, J.W.; Potts, J.R.; Ruoff, R.S. Graphene and graphene oxide: Synthesis, Properties, and Applications. *Adv. Mater.* **2010**, *22*, 3906–3924. [[CrossRef](#)]
70. Chong, J.Y.; Wang, B.; Mattevi, C.; Li, K. Dynamic microstructure of graphene oxide membranes and permeation flux. *J. Membr. Sci.* **2018**, *549*, 385–392. [[CrossRef](#)]
71. Fortunato, E.; Barquinha, P.; Martins, R. Oxide Semiconductor Thin-Film Transistors: A Review of Recent Advances. *Adv. Mater.* **2012**, *24*, 2945–2986. [[CrossRef](#)]
72. Atkinson, J.D.; Fortunato, M.A.; Dastgheib, S.A.; Rostam-Abadia, M.; Rooda, M.J.; Suslick, K.S. Synthesis and characterization of iron-impregnated porous carbon spheres by ultrasonic spray pyrolysis. *Carbon* **2011**, *49*, 587–598. [[CrossRef](#)]
73. Kim, H.; Fortunato, M.E.; Xu, H.; Bang, J.H.; Suslick, K.S. Carbon microspheres as Supercapacitors. *J. Phys. Chem. C* **2011**, *115*, 20481–20486. [[CrossRef](#)]
74. Motuma, B.K.; Matoso, B.J.; Momodu, D.; Oyedotun, K.O.; Coville, N.J.; Manyala, N. Deciphering the Structural, Textural, and Electrochemical Properties of Activated BN-Doped Spherical Carbons. *Nanomaterials* **2019**, *9*, 446. [[CrossRef](#)] [[PubMed](#)]

75. Qiu, H.; Yang, G.; Zhao, B.; Yang, J. Catalyst-free synthesis of multi-walled carbon nanotubes from carbon spheres and its implications for the formation mechanism. *Carbon* **2013**, *53*, 137–144. [[CrossRef](#)]
76. Lobo, L.S. Mechanism of catalytic CNTs growth in 400–650 °C range: Explaining volcano shape Arrhenius plot and catalytic synergism using both Pt (or Pd) and Ni, Co or Fe. *C-J. Carb. Res.* **2019**, *5*, 42. [[CrossRef](#)]



© 2020 by the authors. Licensee MDPI, Basel, Switzerland. This article is an open access article distributed under the terms and conditions of the Creative Commons Attribution (CC BY) license (<http://creativecommons.org/licenses/by/4.0/>).